Recl. Trav. Chim. Pays-Bas 112, 339–346 (1993) 0165–0513/93/06339–08$06.00

α, ω-Dipolar amphiphiles: Influence of rigid and flexible units on aggregation behavior

V. Hessel #, H. Ringsdorf #, R. Laversanne @ and F. Nallet @

Institute of Organic Chemistry, University of Mainz, J.J. Becherweg 18-20, 6500 Mainz, Germany
@ CNRS, Centre de Recherche Paul Pascal, ave. Dr. du Schweitzer, 33600 Pessac, France
(Received December 11, 1992)

Abstract. Mono- and α,ω-dipolar amphiphiles with hydrophilic pyridinium head groups, and flexible and rigid hydrophobic parts have been synthesized. Surface tension and conductivity measurements proved that micellar aggregates for amphiphiles **1–4** are formed. The incorporation of rigid units leads to a decrease in the critical micellar concentration (*CMC*): the rigid monopolar amphiphile **2** aggregates at lower concentration than the flexible monopolar amphiphile **1**. A similar decrease was observed when chain ends were connected: the flexible α,ω-dipolar amphiphile **3** has a lower *CMC* than the flexible monopolar amphiphile **1**. The more flexible amphiphiles **1–3** allow the formation of micelles of different shape leading to both *CMC* and C_t values. For the α,ω-dipolar amphiphile **4** with a rigid azoxybiphenylene core, the possibility of different micellar shapes is reduced, leading only to a *CMC* value ($CMC = C_t$). For the flexible α,ω-dipolar amphiphile **3**, only a small, but linear viscosity increase with concentration is found. Very viscous solutions were measured for the rigid α,ω-dipolar amphiphile **4** above a certain concentration. Phase diagrams of amphiphiles **3** and **4** were determined using polarization-microscopy and X-ray measurements. Flexible α,ω-dipolar amphiphile **3** shows a lyotropic mesophase only at very high concentration (83 mass %). In contrast, rigid analog **4** forms stable lyotropic mesophases at 16 mass %. Both nematic and higher ordered mesophases (probably lamellar) are found for the rigid α,ω-dipolar amphiphile **4**.

Introduction: molecular structure and aggregation behavior of amphiphiles

Amphiphiles are molecules containing hydrophilic and hydrophobic parts. Due to their antagonistic structure they form aggregates in contact with solvents, especially with water[1–4].

The aggregation behavior of amphiphiles is usually complex and depends strongly on their structure and conditions: in diluted solutions, they form spherical, cylindrical and disk-like micelles. Cubic, hexagonal and lamellar lyophases are usually found in more concentrated systems[5–8]. The structure–property relationships of amphiphilic systems are of both theoretical and technological interest and have thus been investigated intensively during recent years (for reviews, see refs.[9–12]).

It was predicted by theory and shown by experiments that amphiphiles containing rigid structures have a simpler aggregation behavior than conventional amphiphiles with flexible hydrophobic chains[13]. In agreement with this, rigid disk-like amphiphiles form only hexagonal lyophases with a columnar order[14,15] and amphiphiles with a fully stretched and stiff alkyl chain, such as perfluorooctanoate, form exclusively lamellar lyophases[16]. Furthermore, amphiphiles with rigid structures (*e.g.*, biphenylene units) seem to favor stable nematic lyophases, which are seldom found for conventional amphiphiles[17].

These examples demonstrate that it is possible, to a certain extent, to control the aggregation behavior of amphiphiles in water via their molecular architecture. In this context, this paper describes the synthesis and phase behavior of amphiphiles containing both flexible and rigid parts (Scheme 1).

These amphiphiles are mono- and α,ω-dipolar, carrying one or two hydrophilic pyridinium headgroups per unit: amphiphile **1** is a conventional amphiphile with one pyridinium headgroup and a flexible alkyl chain of a length of thirteen $-CH_2-$ groups. Seven of these $-CH_2-$ groups are replaced in amphiphile **2** by a rigid mesogenic biphenylene group of the same length. There are two minor shortcomings: namely, the ester units are not at the same position, although the whole molecule is of comparable length. In addition, the biphenylene units in **2** and **4** will show *Π* interactions (see discussion section).

If the monopolar amphiphiles **1** and **2** are covalently linked via their chain ends or an azoxy unit, they yield the α,ω-dipolar amphiphiles **3** and **4**, respectively, with two hydrophilic headgroups. Amphiphile **3** is a flexible α,ω-dipolar amphiphile, whereas **4** contains the very rigid azoxybiphenylene core. In addition, this azoxy group can be photoisomerized and thus allows comparison of the behavior of the cis and trans isomers of **4**. In connection with the question of how the structure and aggregation behavior of mono- and α,ω-dipolar as well as flexible and

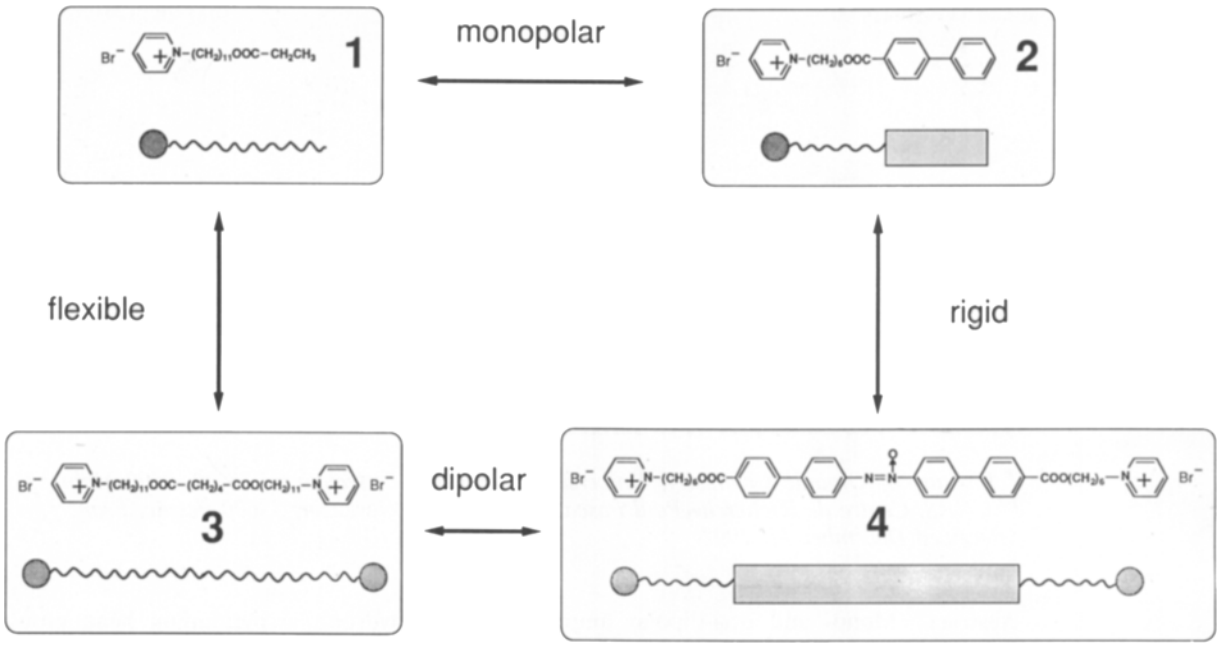

Scheme 1. Mono- and α,ω-dipolar amphiphiles carrying rigid and flexible parts.

rigid amphiphiles are related, the phase behavior of the pyridinium derivatives **1–4** has been studied in aqueous solution.

2. Experimental

2.1. Synthesis of mono- and α,ω-dipolar amphiphiles

The mono- and α,ω-dipolar amphiphiles **1–4** were synthesized via quaternization of the analogous mono- and dibromides with pyridine. For syntheses of the esters **5–8**, mono- or diacid chlorides were esterified either with 11-bromo-1-undecanol or 6-bromo-1-hexanol in THF. The esters were purified via flash chromatography. All esters were quaternized with pyridine in acetonitrile and precipitated in dry ether.

Hexanedioic acid chloride and propionyl chloride were synthesized via standard procedure[18]. The biphenyl-4-carboxylic acid chloride was commercially available (Aldrich).

Hexanedioic acid bis(11-bromoundecyl) ester (**7**), *propionic acid 11-bromoundecyl ester* (**5**) *and biphenyl-4-carboxylic acid 6-bromohexyl ester* (**6**)

Hexanedioic acid chloride (15 g, 82.9 mmol) in 50 ml THF was added dropwise into a solution of 45.8 g (182.3 mmol) 11-bromo-1-undecanol and 16.7 g (165.8 mmol) triethylamine in 100 ml THF. The solution was stirred at room temperature overnight. Solid triethylammonium hydrochloride was filtered off. The clear solution of **7** was evaporated and the crude product was purified by flash chromatography in petroleum-ether/ethyl-acetate, 7:1. The pure product is a white solid; yield 22%.

An analogous procedure was used for **5** (petroleum ether was used as solvent for flash chromatography; yield 87%) and for **6** (dichloromethane was used as solvent for flash chromatography; yield 68%).

7. M.p. 38°C, ^{1}H NMR ($CDCl_3$, 200 MHz, δ/ppm): 1.34 [m, $-COO-CH_2-CH_2-(C\underline{H}_2)_7-$, 28H], 1.68(m, $-CH_2-C\underline{H}_2Br + -CH_2-CH_2-COO-$, 8H) 1.87 (m, $-COO-CH_2-C\underline{H}_2-$, 4H), 2.31 (t, $-C\underline{H}_2-COO-$, 4H), 3.41 (t, $-C\underline{H}_2-Br$, 4H), 4.06 (t, $-COO-C\underline{H}_2-$, 4H). IR(FT-IR, KBr): 1187 (C–O, ν), 1464 (CH_2, δ), 1738 (C=O, ν), 2855 (CH_2, ν_s), 2927 (CH_2, ν_{as}). Anal. calcd. for $C_{28}H_{52}Br_2O_4$: C 54.9, H 8.5, Br 26.6; found: C 54.9, H 8.7, Br 26.2%.

5. Refractive index 1.4606. ^{1}H NMR ($CDCl_3$, 200 MHz. δ/ppm): 1.18 (t, $C\underline{H}_3-CH_2-COO-$, 3H), 1.28 [m, $-COO-CH_2-CH_2-(C\underline{H}_2)_7-$, 14H], 1.62 (m, $-C\underline{H}_2-CH_2Br$, 2H), 1.83 (m, $-COO-CH_2-C\underline{H}_2-$, 2H), 2.32 (q, $CH_3-C\underline{H}_2-COO-$, 2H), 3.40 (t, $-C\underline{H}_2-Br$, 2H), 4.04 (t, $-COO-C\underline{H}_2-$, 2H). IR (FT-IR, KBR): 1179 (C–O, ν), 1496 (CH_2, δ), 1728 (C=O, ν), 2861 (CH_2, ν_s), 2928 (CH_2, ν_{as}). Anal calcd. for $C_{14}H_{27}BrO_2$: C 54.7, H 8.8, Br 25.6; found: C 54.7 H 8.8 Br 26.1%.

6. M.p. 90°C. ^{1}H NMR ($CDCl_3$, 90 MHz, δ/ppm): 1.50 [m, $-COO-CH_2-CH_2-(C\underline{H}_2)_2-$, 4H], 1.80 (m, $-C\underline{H}_2-CH_2-Br$, 2H + m, $-COO-C\underline{H}_2-CH_2-$, 2H), 3.51 (t, $-C\underline{H}_2-Br$, 2H), 4.32 (t, $-COO-C\underline{H}_2-$, 2H), 7.30–8.30 (m, arom., 9H). IR (FT-IR, KBr): 982 (=CH, δ) 1120 (C–O, ν), 1471 (CH_2, δ), 1607 (C=C, ν), 1708 (C=O, ν), 2853 (CH_2, ν_s), 2937 (CH_2, ν_{as}), 3046 (=CH, ν), Anal. calcd. for $C_{19}H_{21}BrO_2$: C 63.2, H 5.8, Br 22.1; found: C 68.6, H 5.7, Br 19.1%.

Propionic acid 11-(1-pyridinio) undecyl ester bromide (**1**), *biphenyl-4-carboxylic acid 6-(1-pyridinio) hexyl ester bromide* (**2**) *and hexanedioic acid bis[11-(1-pyridinio) undecyl] ester dibromide* (**3**)

7 (1.5 g, 2.45 mmol) and 1.9 g (24.51 mmol) pyridine were stirred in 50 ml acetonitrile at 70°C for 7 days. The solution was added dropwise into 500 ml diethyl ether at 0°C. The precipitated white solid was filtered and dissolved in a small amount of water. The aqueous solution of **3** was freeze-dried in vacuum. Yield 80%.

The same procedure was used for **1** (yield 78%) and for **2** (yield 75%).

1. M.p. 35°C. (^{1}H NMR (MeOH-*d*, 200 MHz. δ/ppm): 1.15 (t, $C\underline{H}_3-CH_2-COO-$, 3H), 1.43 [m, $-COO-(CH_2)_2-(C\underline{H}_2)_7-$, 14H], 1.66 (m, $-COO-CH_2-C\underline{H}_2-$, 2H), 2.08 (m, $-C\underline{H}_2-CH_2-N-$, 2H), 2.35 (q, $CH_3-C\underline{H}_2-COO-$, 2H), 4.09 (t, $-COO-C\underline{H}_2-$, 2H) 4.72 (t, $-C\underline{H}_2-N-$, 2H), 8.17 (t, $-N-CH=C\underline{H}-CH-$, 2H), 8,65 (t, $-N-CH=CH-C\underline{H}-$, 1H), 9.09 (d, $-N-C\underline{H}=CH-CH-$, 2H). IR (FT-IR, KBr): 1018 (=CH, δ), 1191 (C–O, ν), 1472 (CH_2, δ), 1629 (C=C, ν), 1737 (C=O, ν), 2854 (CH_2, ν_s), 2926 (CH_2, ν_{as}, 3045(=CH, ν). Anal. calcd. for $C_{19}H_{32}BrNO_2$: C 58.2, H 8.6, N 4.1, Br 20.7; found: C 59.1, H 8.3, N 3.6, Br 19.8%.

2. M.p. 90°C. ^{1}H NMR (MeOH-*d*, 200 MHz, δ/ppm): 1.04 [m, $-COO-(C\underline{H}_2)_2-$, 4H], 1.39 (m, $-COO-CH_2-C\underline{H}_2-$, 2H), 1.87 (m, $-CH_2-CH_2-N-$, 2H), 2.12 (t, $CH_2-C\underline{H}_2-COO-$, 2H), 3.82 (t, $-COO-C\underline{H}_2-$, 2H), 4.52 (t, $-C\underline{H}_2-N-$, 2H), 7.97 (t, $-N-CH=C\underline{H}-CH-$, 2H), 8.44 (t, $-N-CH=CH-C\underline{H}-$, 1H), 8.81 (d, $-N-C\underline{H}=CH-CH-$, 2H). IR (FT-IR, KBr): 979 (=CH, δ), 1167 (C–O, ν) 1470 (CH_2, δ), 1636 (C=C, ν), 1729 (C=O, ν), 2851 (CH_2, ν_s), 2963 (CH_2, ν_{as}), 3016 (=CH, ν). Anal. calcd. for $C_{24}H_{26}Br\,NO_2$: C 65.5, H 5.9, N 3.2, Br 20.7; found: C 63.5, H 5.9, N 3.2, Br 18.2%.

3. M.p. 35°C. ^{1}H NMR (D_2O, 200 MHz, δ/ppm): 1.04 [m, $-COO-(CH_2)_2-(C\underline{H}_2)_7-$, 28H], 1.39 (m, $-COO-CH_2-C\underline{H}_2-$, 4H), 1.87 (m, $-C\underline{H}_2-CH_2-N-$, 4H), 2.12 (t, $-CH_2-C\underline{H}_2-COO-$, 4H), 3.82 (t, $-COO-C\underline{H}_2-$, 4H), 4.52 (t, $-CH_2-N-$, 4H), 7.30–7.90 (m, arom., 9H), 7.97 (t, $-N-CH=C\underline{H}-CH-$, 4H), 8.44 (t, $-N-CH=CH-C\underline{H}-$, 2H), 8.81 (d, $-N-C\underline{H}=CH-CH-$, 4H). IR (FT-IR, KBr): 979 (=CH, δ), 1167 (C–O, ν), 1470 (CH_2, δ), 1636 (C=C, ν), 1729 (C=O, ν), 2851 (CH_2, ν_s), 2963 (CH_2, ν_{as}), 3016 (=CH, ν), Anal. calcd. for $C_{38}H_{62}Br_2N_2O_4$: C 59.2, H 8.1, N 3.7, Br 20.8; found: C 58.7, H 8.1, N 4.0, Br 18.9%.

4',4''' -Azoxybis [biphenyl-4-carbonyl chloride]

Synthesis was carried out using a method previously described[19]. 4',4'''-Azoxybis [biphenyl-4-carbonyl acid] (21.1 g, 50 mmol, Casella, Frankfurt) was reacted with 22.9 g (110 mmol) phosphorus pentachloride and 150 ml phosphorus oxychloride. After stirring for 4 h, the solution was heated to 60°C and a few drops DMF were added. The reaction mixture did not become homogenous. The hot suspension was filtered and the filtrate was allowed to crystallize. The crude product was recrystallized twice from absolute xylene. The acid dichloride forms yellow needles; yield 20%. IR (FT-IR, KBr): 1601 (C=C, ν), 1777 (C=O, ν).

4',4'''-Azoxybis [biphenyl-4-carboxylic acid 6-bromohexyl ester] (**8**)

The reaction was carried out similar to that used for the synthesis of **7**. *o*-Dichlorobenzene was used as solvent instead of THF. The crude product was purified by flash chromatography with dichloromethane as solvent. The product is a yellow solid; yield 38%; M.p. 230°C (dec.). ^{1}H NMR ($CDCl_3$, 200MHz. δ/ppm): 1.51 [m, $-COO-CH_2-CH_2-(C\underline{H}_2)_2-$, 8H], 1.86 (m, $-C\underline{H}_2-CH_2-Br$, 4H), 1.92 (m, $-COO-CH_2-C\underline{H}_2-$, 4H), 3.47 (t, $-C\underline{H}_2-Br$, 4H), 4.37 (t, $-COO-CH_2-$, 4H), 7.72 (d, arom., 8H), 8.12 (d, arom., 4H), 8.37 (dd, arom., 4H). IR (FT-IR, KBr): 979 (=CH, δ), 1199 (C-O, ν), 1455 (CH_2, δ), 1795 (C=O, ν), 2857 (CH_2, ν_s), 2941 + 2957 (CH_2, ν_{as}), 3053 (=CH, ν). Anal. calcd. for $C_{38}H_{40}Br_2N_2O_5$: C 59.7, H 5.2, N 3.7, Br 20.9; found: C 59.8, H 5.4, N 3.7, Br 20.4%.

4',4'''-Azoxy [biphenyl-4-carboxylic acid 6-(1-pyridiniohexyl) ester] dibromide (**4**)

The same procedure as for amphiphiles **1**, **2** and **3** was used. The product is a yellow solid; yield 88%; m.p. 230°C (dec). ^{1}H NMR (DMSO-d_6 200 MHz, δ/ppm): 1.42 [m, $-COO-CH_2-CH_2-(C\underline{H}_2)_2-$, 8H], 1.74 (m, $-COO-CH_2-C\underline{H}_2-$, 4H), 2.02 (m, $-C\underline{H}_2-CH_2-N=$, 4H), 4.30 (t, $-COO-C\underline{H}_2-$, 4H), 4.70 (t, $-C\underline{H}_2-N=$, 4H), 7.72 (d, arom., 8H), 8.12 (d, arom., 4H), 8.37 (dd, arom., 4H), 8.20 (t, -N-CH=C<u>H</u>-CH-, 4H), 8.67 (t, -N-CH=CH-CH2a-y-, 2H), 9.20 (d, -N-C<u>H</u>=CH-CH, 4H). IR (FT-IR, KBr): 998 (=CH, δ), 1182 (C-O, ν), 1458 (CH_2, δ), 1634 (C=C, ν), 1705 (C=O, ν), 2856 (CH_2, ν_s), 2937 (CH_2, ν_{as}), 3046 (=CH, ν). Anal. calcd. for $C_{48}H_{50}Br_2N_4O_5$: C 62.4, H 5.4, N 6.1 Br 17.4; found: C 62.0, H 5.5, N 6.0 Br 17.6%.

2.2. Measurements

Surface-tension measurements were made with a Tensiometer (Lauda TE 1 C/2 with SAE + KM3) using the ring method. Two or three stock solutions were diluted to give fifteen to twenty solutions.
Conductivity measurements were made with a conductometer (Methrom 660 series 01) with a platinum electrode (6.098.110, constant c 0.76 cm^{-1}). A stock solution of 15 ml was diluted ten fold with 1 ml pure water. Water (10 ml) was then removed and the solution was diluted again as ten fold. This procedure was repeated several times until very dilute concentrations were achieved. Viscosity measurements were made with a capillar viscosimeter (Schott 53810) at 28°C. Several stock solutions were prepared by dilution of one stock solution. The very viscous solutions (> 7 mass%) were diluted directly inside the viscosimeter.
Light-scattering measurements were made with an AMTEC light-scattering system, using a Kr^+ laser operating at 647.1 nm. The solutions were centrifuged for $\frac{1}{2}$ h at 4000 revs./ min to prevent dust. The intensity of the scattered light was measured at a fixed angle several times to get an average value.

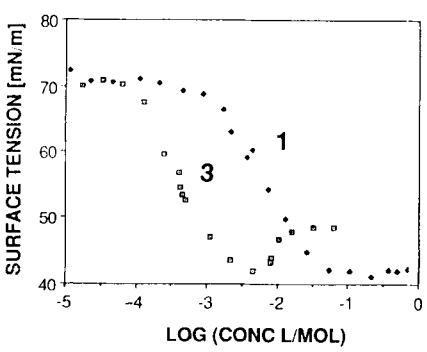

Fig. 1. Surface-tension measurements of flexible monopolar amphiphile **1** *(♦) and flexible α,ω-dipolar amphiphile* **3** *(□).*

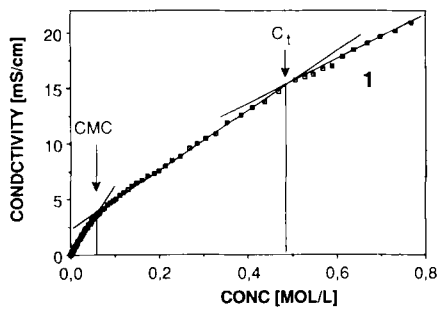

Fig. 2. Conductivity measurement of flexible monopolar amphiphile **1**.

Phase diagrams were made by polarization-microscopy investigations (microscope: Ortholux POL-BK, Leitz; camera: MPS 11, Wild; heating unit: FP 52, Mettler) on sealed samples. The different samples were prepared from a concentrated stock solution by dilution with water. The concentrations of the dilute solutions were determined by gravimetric control. Small amounts of the sample were brought between two microscopy slides, which were sealed with a two-component glue. (This glue is not water soluble and is heat-resistant below 200°C.) The textures gave a first orientation of the structure of the lyotropic mesophases, but detailed analysis was only possible by X-ray measurements. To allow statistical calculations several heating and cooling cycles of the samples were made.
X-ray measurements were made on a home-made camera (Cu rotating anode operating at 18 kW; graphite monochromator set to λ 1.54 Å; slit collimation). It was not possible to transfer the samples into a capillary, because they were too viscous. Therefore, the samples were held in a sample holder by adhesive tape (Tesa film), which had previously been tested for showing no signal in the wave vector explored. Measurement was made immediately after preparation of the sample to avoid evaporation of water. By repeating the measurements after one or two days, it was shown that no evaporation had occurred.

3. Results and discussion

3.1. Micellar solutions of flexible mono- and α,ω-dipolar amphiphiles **1** *and* **3**

The micellar behavior of the amphiphiles **1**–**4** was characterized from surface tension and conductivity measurements. A break in the slope of the plot of the conductivity[20] or surface tension[21] vs. concentration is usually assigned to the formation of micelles (*CMC*: critical micellar concentration). A second break is assigned to a change in the shape of micelles (C_t: transition concentration)[20].
Figure 1 shows a surface-tension plot of the flexible monopolar amphiphile **1** and the flexible α,ω-dipolar amphiphile **3**. The *CMC* value is significantly lower for the α,ω-dipolar amphiphile **3** ($4.3 \cdot 10^{-3}$ mol/l) than for the monopolar amphiphile **1** ($3.9 \cdot 10^{-2}$ mol/l). Chain-end linkage of two monopolar amphiphiles seems to lead to micellar aggregation at dilute concentrations, at which the monopolar amphiphile still does not form aggregates. This

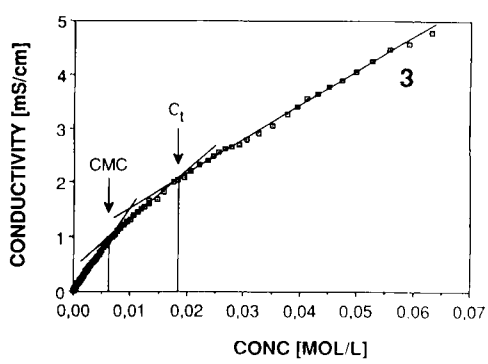

Fig. 3. Conductivity measurement of flexible α,ω-dipolar amphiphile **3**.

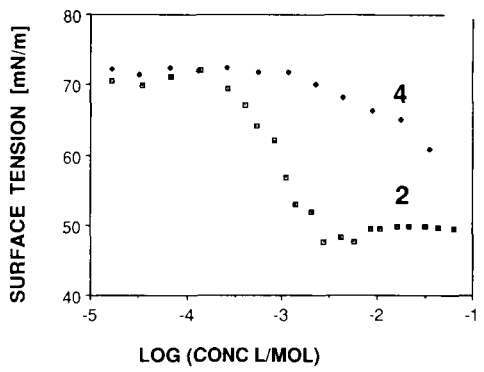

Fig. 4. Surface-tension measurements of rigid monopolar amphiphile **2** *(□) and rigid α,ω-dipolar amphiphile* **4** *(◆).*

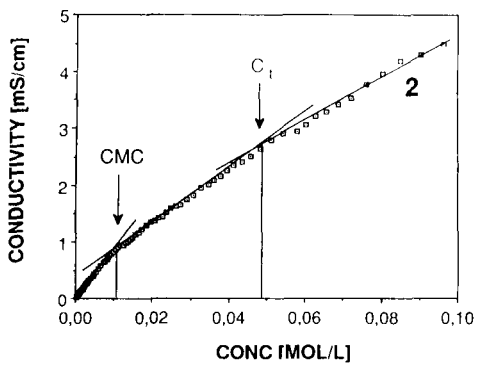

Fig. 6. Conductivity measurement of rigid monopolar amphiphile **2**.

type of stabilization of micelles for α,ω-dipolar amphiphiles has been reported earlier[22]. Doubling of the chain length seems to have a larger influence on the aggregation behavior than doubling of the number of headgroups[8,12,23,24].

The conductivity measurement (Figure 2) of amphiphile **1** shows two transitions, *CMC* at $5.3 \cdot 10^{-2}$ mol/l and in addition C_t at $4.9\ 10^{-1}$ mol/l. The *CMC* values measured by surface tension and conductivity are comparable. The difference can be related to the fact that micelle formation at a defined concentration (*CMC*) is an oversimplification[25], especially for amphiphiles carrying two headgroups and/or rigid units. It is known that micelles, in general, are formed only within a certain concentration range. Thus, the higher *CMC* values from conductivity measurements reflect the end of micelle formation, whereas those from surface tension show the beginning. Aggregation of amphiphiles **1–4** seems to be a compromise between continuous stepwise self-association and micellar formation of narrow-size distribution (according to the definition of *Mukerjee*[26]).

The C_t of amphiphile **1** at higher concentrations can be related to a change in the shape of the micelles, probably from spherical to cylindrical or plate-like micelles.

Figure 3 shows the conductivity measurement of the α,ω-dipolar flexible amphiphile **3**. As for the monopolar amphiphile **1**, both a *CMC* ($5.6 \cdot 10^{-3}$ mol/l) and a C_t ($2.0 \cdot 10^{-2}$ mol/l) were found. Compared to **1**, however, both values are shifted to lower concentration, the C_t value is especially shifted to much lower concentration (see Table 1). This point to the fact that the α,ω-dipolar amphiphile **3** has a higher tendency to form higher ordered aggregates in aqueous solutions.

The formation of lamellar lyophases (see section 3.4) of amphiphiles **3** and **4** underlines that these aggregates are plate-like (and not cylindrical) micelles. Another argument that plate-like micelles exist is the number of free counter-ions which is much lower for the rigid amphiphile **4** (27%) than for the flexible amphiphile **2** (65%) (see section 3.2). This number can be calculated from the slope of the conductivity vs. concentration plot, before and after the *CMC*. The high number of bound counterions forces the headgroups to stay closer together, as expected for plate-like micelles.

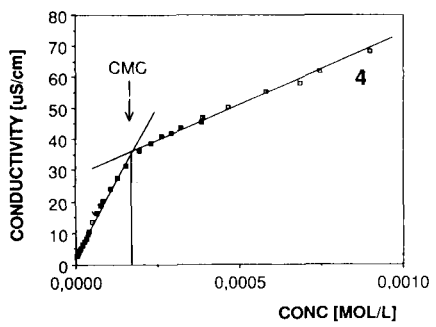

Fig. 5. Conductivity measurement of rigid α,ω-dipolar amphiphile **4**.

3.2. Micellar solutions of rigid mono- and α,ω-dipolar amphiphiles **2** *and* **4**

A comparison of the aggregation behavior of the monopolar amphiphile **2** and the α,ω-dipolar amphiphile **4** yields information on the influence of the replacement of flexible units by rigid units in addition to insight into the difference between these rigid amphiphiles. Figure 4 shows the surface-tension measurement for rigid amphiphiles **2** and **4**.

The *CMC* of the rigid monopolar amphiphile **2** is lower ($5.6 \cdot 10^{-3}$ mol/l) than for the corresponding flexible monopolar amphiphile **1** ($3.9 \cdot 10^{-2}$ mol/l). This is due to the fact that the rigid biphenylene system has less degrees of freedom in solution. Furthermore, the aromatic rings may interact via dispersion forces and help to stabilize the aggregate. Thus, both chain-end linkage, as in **3**, and the introduction of rigid units, as in **2**, leads to formation of micelles at lower concentrations.

The rigid α,ω-dipolar amphiphile **4** exhibits, as expected, unusual surface-tension behavior: no plateau of surface tension at high concentrations is detectable until a high concentration; the surface activity is also very low. The latter aspect has been reported for several multipolar amphiphiles[27]. In case of **4**, it is a consequence of the very unfavorable orientation of the α,ω-dipolar rigid amphiphile **4** at the air–water surface. It is also interesting to note that the area of the molecules occupied at the air–water interface for amphiphiles **1–4** can be calculated from the slope in the surface tension *vs.* logarithm of concentration plots[11] (in Figures 1 and 4). Whereas the molecular areas are 90 Å^2 for **1** and 89 Å^2 for **2**, a larger area of 128 Å^2 is found for **3**. This is in agreement with the area needed for a α,ω-dipolar amphiphile[11]. Again, an extremely high value is found for the rigid α,ω-dipolar amphiphile **4** (406 Å^2), caused by the fact that this molecule is unable to be bent.

Conductivity measurements show only one transition ($CMC = C_t$) at $1.7 \cdot 10^{-4}$ mol/l (Figure 5) for the rigid α,ω-dipolar amphiphile **4**. At this concentration, the sur-

Table 1 CMC, C_t and σ_{CMC} of the amphiphiles **1–4**.

Amphiphile	*CMC* [mol/l]		C_t [mol/l] Conductivity	σ_{CMC} [mN/m]
	Surface tension	Conductivity		
1	$3.9 \cdot 10^{-2}$	$5.3 \cdot 10^{-2}$	$4.9 \cdot 10^{-1}$	42
2	$5.6 \cdot 10^{-3}$	$1.1 \cdot 10^{-2}$	$4.8 \cdot 10^{-2}$	48
3	$4.3 \cdot 10^{-3}$	$5.6 \cdot 10^{-3}$	$2.0 \cdot 10^{-2}$	49
4	–	$1.7 \cdot 10^{-4}$	–	65

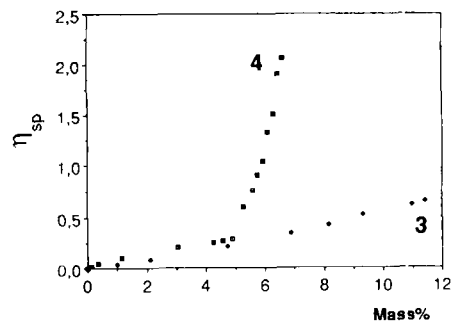

Fig. 7. Measurement of specific viscosity versus mass% of α,ω-dipolar flexible amphiphile **3** *(♦) and rigid α,ω-dipolar amphiphile* **4** *(□).*

face-tension measurement is not able to reflect any micellar aggregation. That means that there are hardly any molecules at the surface, while micelles already exist in solution. The $CMC = C_t$ value ($1.7 \cdot 10^{-4}$ mol/l) is much lower (nearly two orders of magnitude) than for the rigid monopolar analog **2** ($1.1 \cdot 10^{-2}$ mol/l) and also lower than for the flexible α,ω-dipolar analog **3** ($5.6\ 10^{-3}$ mol/l) (see Figures 3 and 5). A second break corresponding to an additional transition is not detectable in the conductivity measurement (even at concentrations as high as $3.5 \cdot 10^{-2}$ mol/l), not shown in Figure 5. This is an indication that amphiphile **4** does not form spherical micelles, but directly forms higher aggregates (probably plate-like). The formation of plate-like micelles is a direct consequence of the rigid structure of the amphiphile, which does not allow any bending of the molecule.

In contrast to the behavior of **4**, conductivity measurement of the monopolar amphiphile **2** (Figure 6) shows both a *CMC* ($1.1 \cdot 10^{-2}$ mol/l) and a C_t ($4.8 \cdot 10^{-2}$ mol/l). Again, the *CMC* value measured by conductivity is higher than the analogous value measured by surface tension (see Table 1). Compared to the monopolar flexible amphiphile **1**, both the *CMC* and the C_t value of the rigid monopolar amphiphile **2** are significantly shifted to lower concentrations.

The *CMC* and C_t values of amphiphiles **1–4** are summarized in Table 1. Two general tendencies can be deduced from both the surface-tension and conductivity measurements of amphiphiles **1–4**: the *CMC* and C_t values decrease in the direction from the flexible monopolar amphiphile **1** to the rigid monopolar **2** to the flexible α,ω-dipolar **3** to the rigid α,ω-dipolar **4**.

The surface activity (surface tension at the *CMC*) decreases similarily from the flexible monopolar amphiphile **1** (42 mN/m) to the flexible α,ω-dipolar **3** (48 mN/m) to the rigid monopolar **2** (49 mN/m) to the rigid α,ω-dipolar amphiphile **4** (65 mN/m).

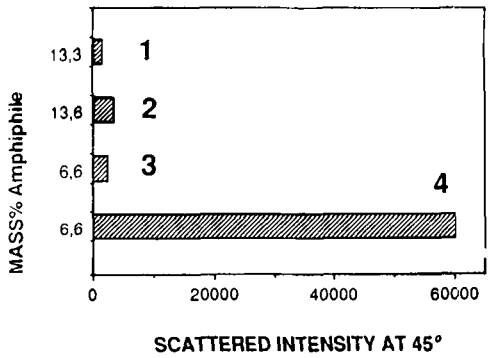

Fig. 9. Measurement of intensity of scattered light at fixed angle of 45° for mono- and α,ω-dipolar amphiphiles **1–4** *at similar concentrations.*

3.3. Gel formation of rigid α,ω-dipolar amphiphile **4**

The obtain more information on the concentration-dependent aggregation behavior of the flexible α,ω-dipolar amphiphile **3** and its rigid analog **4**, the viscosity of their solutions was measured. It was expected that the formation of anisotropic and probably plate-like micelles would have a strong influence on the viscosity of concentrated aqueous solutions[28]. The specific viscosity of the rigid α,ω-dipolar amphiphile **4** is, in fact, higher compared to the flexible α,ω-dipolar amphiphile **3** over the whole concentration range (Figure 7). However, the most remarkable finding is that the viscosity of **4** does not increase homogenously, but shows a strong deviation from linearity at 5 to 6 mass%. This indicates an overlap of elongated micellar aggregates, leading to gel formation.

This finding is confirmed by light-scattering measurements of **4**, showing that the composition dependency of the scattered intensity at a fixed angle (45 and 90°) shows comparable behavior to that of the viscosity (figure 8). The gyration radius and, therefore, the length of the micelles increases with concentration. At 6–7 mass%, the intensity of scattered light increases greatly (similar to the viscosity measurement). This fact shows that the dimensions of the aggregates still increase in the gel.

This increase of viscosity and of the intensity of the scattered light can be explained by growth of the micelles, leading to a higher gyration radius. This is supported by the fact that the absolute amount of scattered light at fixed angle and fixed concentration is much higher for the

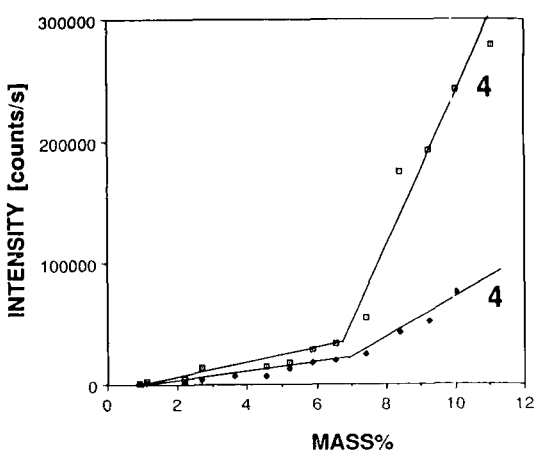

Fig. 8. Measurement of intensity of scattered light at 45° (♦) and 90° (□) versus mass% of rigid α,ω-dipolar amphiphile **4** *(lines are only guides for the eye and do not indicate a linear relationship).*

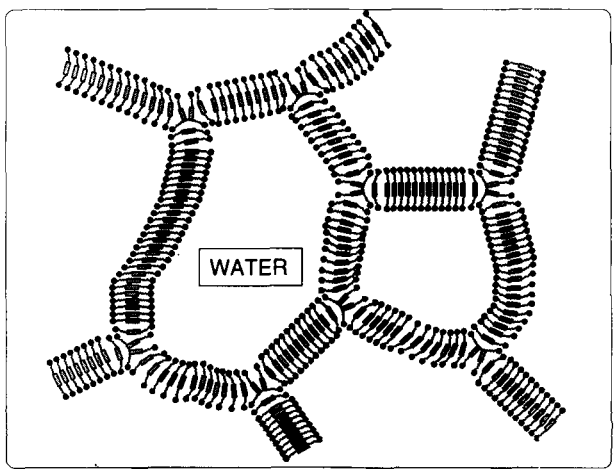

Fig. 10. Cross section through three-dimensional zeolith-type network of rigid α,ω-dipolar amphiphile **4** *at concentrations higher than 6 mass%.*

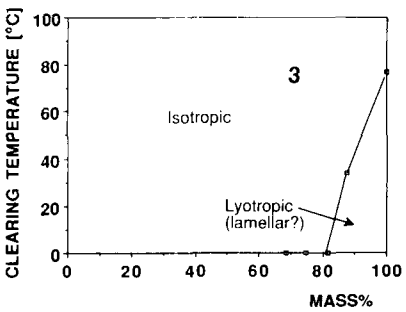

Fig. 11. Phase diagram of flexible α,ω-dipolar amphiphile **3**.

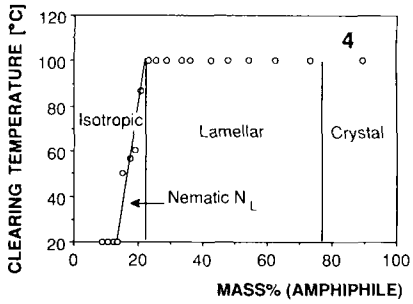

Fig. 13. Phase diagram of rigid α,ω-dipolar amphiphile **4**.

α,ω-dipolar rigid amphiphile **4** than for amphiphiles **1**, **2** and **3** (see Figure 9).

Three-dimensional networks (gels) of amphiphilic aggregates are known for cylindrical micelles and for vesicles[20]. However vesicular structures do not increase in size upon gel formation and show, therefore, no increase in the intensity of scattered light with concentration. On the other hand, the formation of cylindrical micelles is unlikely for the rigid amphiphile **4** because of its linear shape. In addition, they usually show an even higher viscosity increase. As far as the structure of the gels is concerned, we can only speculate: certain it is only that it must be a three-dimensional network of plate-like micelles. If we assume that three plate-like micelles form the netpoints, the result would be a continous lamellar network surrounding water caves, as schematically shown in Figure 10. Further investigations will be necessary to elucidate the correct structure.

3.4. Lyotropic mesophases for α,ω-dipolar amphiphiles **3** *and* **4**

Lyotropic mesophases at room temperature were found for the two α,ω-dipolar amphiphiles **3** and **4** via polarization microscopy (using both contact and evaporation techniques). The two monopolar amphiphiles **1** and **2** were not examined, but are expected to show a small lyotropic mesophase region at high concentration.

The phase diagram for the flexible α,ω-dipolar amphiphile **3** is given in Figure 11.

Lyotropic mesophases of **3** are stable only for a small region at high concentration of the amphiphile. For all concentrations lower than 86 mass%, only isotropic solutions were found (no birefringence between crossed polarizers).

X-ray measurement of the lyotropic mesophase of amphiphile **3** at 91 mass% clearly shows its lamellar structure (Figure 12): four peaks were found: their wave vectors are in the order of n times the wave vector of the first peak (n is the number of the peaks). The distance of 39 Å, which is calculated for the first-order peak by the Bragg equation, corresponds well to a tilted lamellar structure. The small half-width of the peaks is an indication that the structure may be the higher ordered L_β structure instead of the usual L_α structure. The complex intensity distribution (the intensity of the fourth order peak is higher than the intensity of the second-order peak) is a consequence of the complex scattering-length density profile of the amphiphile **3**.

The phase diagram for the rigid α,ω-dipolar amphiphile **4** is totally different compared to that of the flexible α,ω-dipolar amphiphile **3** (Figure 13): the lyotropic mesophase is stable over a wide temperature (> 100°C) and concentration range of the amphiphile (16–80 mass%). This is typical behavior for amphotropic compounds combining lyotropic and thermotropic liquid-crystal properties[29] due to the amphiphilic and mesogenic molecular structure. According to texture analysis, the mesophase was assigned as lamellar[30]. For concentrations higher than 82 mass%, the amphiphile–water mixture is only crystalline. Figure 14 represents a X-ray measurement for a 32 mass% sample of the amphiphile **4**. One very intense peak was found at low wave-vector, and one amorphous halo at wide wave-vector. It is suprising not to find higher orders of such an intense peak. The distance of 80 Å calculated by the Bragg equation is too small for a lamellar structure with about 70 mass% water between the layers. Thus, the intense peak is probably not the first-order peak, but may be second-order. Other X-ray measurements (not shown) for similar amphiphiles have always shown Bragg distances, that were half the value expected for a lamellar structure. Thus, for these kinds of multipolar amphiphiles, first-order peaks may vanish due to the high symmetry of the electronic-density distribution of the amphiphile.

Since no peaks of higher order were detected, it is not possible to determine the structure of the mesophase directly from one X-ray measurement. Therefore, four X-ray measurements at different concentrations were made. The Bragg distances calculated from these measurements *vs.* 1/mass% show a linear relationship, as expected for a lamellar structure (Figure 15).

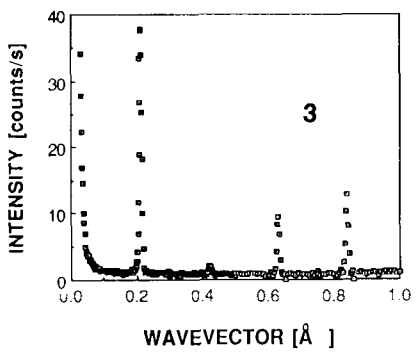

Fig. 12. X-ray measurement of 91 mass% sample of flexible α,ω-dipolar amphiphile **3** *(low angle).*

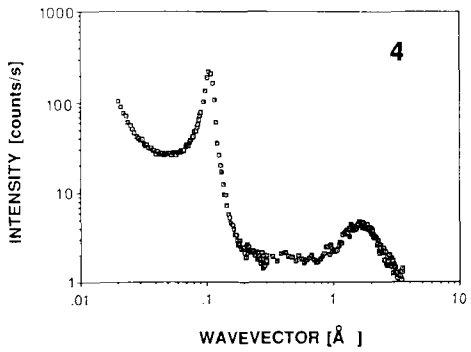

Fig. 14. X-ray measurement of 32 mass% sample of rigid α,ω-dipolar amphiphile **4**: *low-and wide-angle plot (double logarithmic).*

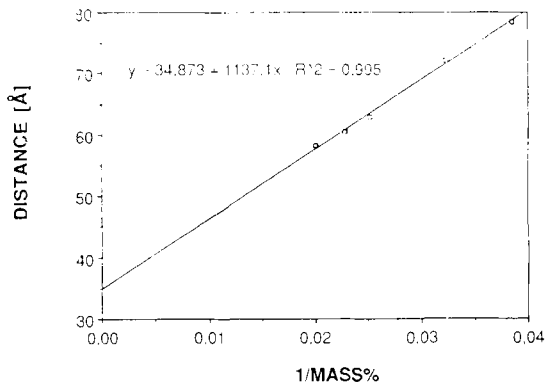

Fig. 15. Plot of calculated distances (from X-ray measurements at different concentrations) vs. 1/mass% of rigid α,ω-dipolar amphiphile **4**.

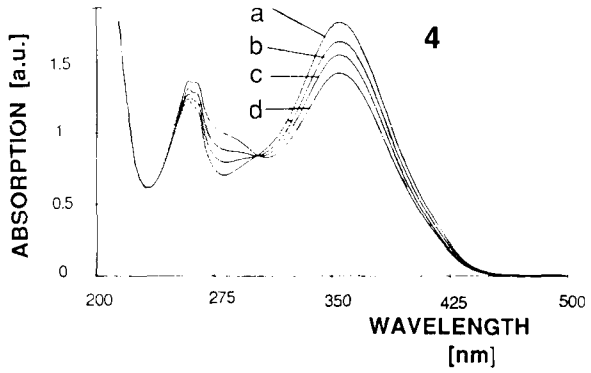

Fig. 17. UV measurements of rigid α,ω-dipolar amphiphile **4**: *Change of UV-absorption upon irradiation due to trans-to-cis isomerization. a: 0 minutes, b: 15 seconds, c: 1 minute, d: 2 minutes.*

The mesophase of amphiphile **4** at concentrations above 23 mass% has a mosaic texture, which is typical for the lamellar orientation (Figure 16)[30].

3.5 Influence of photoinduced cis–trans-isomerization on stability of mesophase

The rigid α,ω-dipolar amphiphile **4** contains a mesogenic azoxy group, that can undergo photoinduced *cis–trans* isomerization leading to the non-mesogenic cis unit. Figure 17 shows the change in the UV absorption in water upon irradiation with a xenon–mercury high-pressure lamp. The isosbestic points indicate that only one photoprocess occurs.

Both the nematic and the lamellar mesophase were irradiated. While the lamellar mesophase was stable on irradiation for hours, the nematic mesophase was transferred to the isotropic solution after 15 minutes irradiation. Figure 18 shows an irradiated and a non-irradiated part of the nematic mesophase.

The non-irradiated lyotropic mesophase and irradiated isotropic solution are clearly divided. Due to thermal rearrangement, the irradiated isotropic solution formed a nematic lyophase again after relaxation for one day. Thus, the whole photoprocess is reversible.

Conclusions

It could be shown that the multipolar amphiphiles **1–4** are able to aggregate to micelles. The α,ω-dipolar amphiphiles **3** and **4** aggregate to micelles at significant lower concentrations than monopolar amphiphiles **1** and **2**. The *CMC* of the rigid amphiphiles **2** and **4** is lower than the *CMC* for flexible amphiphiles **1** and **3**. Thus both chain-end linkage and the introduction of rigid parts leads to stabilization of the micellar solution.

The more flexible amphiphiles **1–3** can undergo a change in micellar shape (C_t) with increasing concentration, as known for conventional monopolar amphiphiles. The C_t value of the α,ω-dipolar amphiphile **3** is lower than the value for the monopolar amphiphile **1** (similar behavior to the *CMC* value). The rigid amphiphile **4** forms only one type of micelles. Analysis of the textures of the lyophases, the low dissociation degree of the counter-ions in the micelles and the enormous increase of viscosity with increasing concentration indicate that this shape is plate-like.

The surface activity of amphiphiles **1–4** depends strongly on the possible orientation of the molecule at the air-water interface. Introduction of rigid parts and chain-end linkage both cause an unfavorable orientation and, thus, decrease the surface activity.

Solutions of the α,ω-dipolar rigid amphiphile **4** become very viscous at 5 mass%, which is a consequence of overlap of micellar aggregates. The flexible, α,ω-dipolar amphiphile **3** does not show this behavior. The scattered-light intensity increases similarly with increasing concentration. This is an indication of elongated aggregate structures, which form a three-dimensional network (gel).

Lyotropic mesophases are found for both α,ω-dipolar amphiphiles **3** and **4**. The stability of the lyotropic mesophases with respect to temperature and concentration increases strongly from the flexible amphiphile **2** to the rigid amphiphile **4**. This is due to introduction of the mesogenic parts for amphiphile **4**. Texture analysis and X-ray measurements confirm a tilted lamellar structure (L_β phase) for the rigid, α,ω-dipolar amphiphile **3**. X-ray measurements at different concentrations of the am-

Fig. 16. (a) Mosaic texture of lamellar mesophase of rigid α,ω-dipolar amphiphile **4** *(23–82 mass%, upper part), (b) Schlieren texture of nematic mesophase of rigid α,ω-dipolar amphiphile* **4** *(16–23 mass%, lower part).*

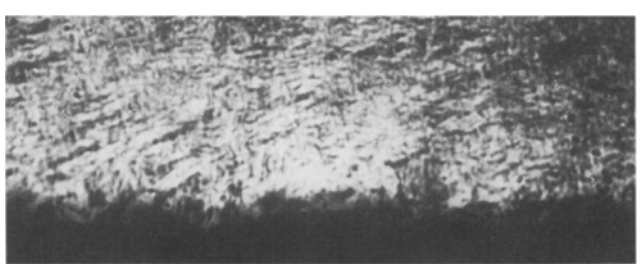

Fig. 18. Irradiation of nematic mesophase of rigid α,ω-dipolar amphiphile **4**: *upper part: irradiated, lower part: protected from irradiation.*

phiphile **4** and texture analysis prove a lamellar structure. Photoisomerization allows switching from the nematic mesophase of the amphiphile **4** to an isotropic micellar solution.

References

1 *D. W. R. Gruen*, Progr. Colloid & Polymer Sci **70**, 6 (1985).
2 *D. Fennell Evans* and *B. W. Ninham*, J. Phys. Chem. **90**, 226 (1986).
3 *J. Mitchell* and *B. W. Ninham*, J. Chem. Soc., Faraday Trans 2 **77**, 601 (1981).
4 *P. Fromherz*, Ber. Bunsenges. Phys. Chem. **85**, 891 (1981).
5 *H. Hoffmann*, Ber. Bunsenges. Phys. Chem. **88**, 1078 (1984).
6 *G. J. T. Tiddy* and *M. F. Walsh*, "Lyotropic liquid crystals, Aggregation: Aggregation processes in solutions, Studies in physical and theoretical chemistry", **26**, Chapter 7, p. 151 (1983), Amsterdam.
7 *K. Fontell*, Colloid Polymer Sci. **268**, 264 (1990).
8 *A. Saupe*, J. Colloid Interf. Sci. **58**, No. 3, 549 (1977).
9 *S. M. Hamid, D. C. Sherrington* and *C. J. Suckling*, Colloid & Polymer Sci **264**, 883 (1986).
10 *J. C. Brackman* and *J. B. F. N. Engberts*, Langmuir **7**, 46 (1991).
11 *S. K. Abid, S. M. Hamid* and *D. C. Sherrington*, Colloid and Interf. Sci. **120**, (1) 245 (1987).
12 *R. Zana, S. Yiv* and *K. M. Kale*, J. Colloid and Interf. Sci. **77** (2), 456, (1986).
13 *M. P. Taylor* and *J. Herzfeld*, Langmuir **6**, 911 (1990).
14 *N. Boden, R. J. Bushby, C. Hardy* and *F. Sixl*, Chem. Phys. Lett. **123**, (5), 359 (1986).
15 *R. Keller-Griffith, H. Ringsdorf* and *A. Vierengel*, Colloid & Polymer Sci. **264**, 924 (1986).
16 *N. Boden, S. A. Corne* and *K. W. Jolley*, Chem. Phys. **105**, (1) (1984).
17 *B. Lühmann, H. Finkelmann* and *G. Rehage*, Makromol. Ch. **186**, 1059 (1985).
18 "Organikum", 16. edition, VEB Deutscher Verlag der Wissenschaften, Berlin 1986, p. 423.
19 *W. Kreuder, H. Ringsdorf, O. Hermann-Schönherr* and *J. H. Wendorff*, Angew. Chem. Intern. Ed. Engl. **26**, 1249 (1987).
20 *H. Hoffmann, G. Platz, H. Rehage, W. Schorr* and *W. Ulbricht*, Ber. Bunsenges. Phys. Chem **85**, 255 (1981).
21 *R. Heusch*, Tenside **21**, 173 (1984).
22 *M. Yasuda, K. Ikeda, K. Esumi* and *K. Meguro*, Bull. Chem. Soc. Jpn. **62**, 3648 (1989).
23 *C. Bunton, C. A. Robinson, L. J. Schaak* and *M. F. Stam*, J. Org. Chem. **36**, 2346 (1971).
24 *K. Shinoda, T. Nakagawa, B. Tamamushi* and *T. Isemura*, "Colloidal surfactants", Academic press, New York 1963.
25 *P. H. Elworthy* and *K. J. Mysels*, J. Colloid Interface Sci. **21**, 331 (1966).
26 *P. Mukerjee*, J. Pharm. Sci. **63**, 972 (1974).
27 *F. M. Menger, M. Takeshita* and *J. F. Chow*, J. Am. Chem. Soc. **103**, 5938 (1981).
28 *H. Hoffmann, H. Rehage, G. Platz, W. Schorr, H. Thurn* and *W. Ulbricht*, Colloid & Polymer Sci. 1042 (1982).
29 *S. Fuller, J. Hopwood, A. Rahman, N. Shinde, G. J. Tiddy, G. S. Attard, O. Howell* and *S. Sproston*, Liquid crystals **12** (3), 521 (1992).
30 *F.B. Rosevaer*, J. Am. Chem. Soc. **31**, 628 (1954).